

# Automated spray coating process for the fabrication of large-area artificial opals on textured substrates

Alexander N. Sprafke,<sup>1</sup> Daniela Schneevoigt,<sup>1,\*</sup> Sophie Seidel,<sup>1</sup> Stefan L. Schweizer,<sup>1</sup> and Ralf B. Wehrspohn<sup>1,2</sup>

<sup>1</sup> Institute of Physics, Martin-Luther-University Halle-Wittenberg, Germany

<sup>2</sup> Fraunhofer Institute for Mechanics and Materials IWM, Halle, Germany

\*[daniela.schneevoigt@physik.uni-halle.de](mailto:daniela.schneevoigt@physik.uni-halle.de)

**Abstract:** 3D photonic crystals, such as opals, have been shown to have a high potential to increase the efficiency of solar cells by enabling advanced light management concepts. However, methods which comply with the demands of the photovoltaic industry for integration of these structures, i. e. the fabrication in a low-cost, fast, and large-scale manner, are missing up to now. In this work, we present the spray coating of a colloidal suspension on textured substrates and subsequent drying. We fabricated opaline films of much larger lateral dimensions and in much shorter times than what is possible using conventional opal fabrication methods.

© 2013 Optical Society of America

**OCIS codes:** (050.5298) Diffraction and gratings - Photonic crystals; (160.5298) Materials - Photonic crystals; (310.1860) Thin films - Deposition and fabrication; (310.6845) Thin films - Devices and applications; Light management in solar cells.

---

## References and links

1. E. Yablonovitch, "Inhabited spontaneous emission in solid-state physics and electronics," *Phys. Rev. Lett.* **58**(20), 2059–2062 (1987).
2. S. John, "Strong localization of photons in certain disordered dielectric superlattices," *Phys. Rev. Lett.* **58**(23), 2486–2489 (1987).
3. M. Peters, A. Bielawny, B. Bläsi, R. Carius, S. W. Glunz, J. C. Goldschmidt, H. Hauser, M. Hermle, T. Kirchartz, P. Löper, J. Üpping, R. B. Wehrspohn, and G. Willeke, *Photonic Concepts for Solar Cells in Physics of Nanostructured Solar Cells* (V. Badescu, and M. Paulescu, eds., Nova Science Pub, Inc., 2009), pp. 1–42.
4. A. N. Sprafke and R. B. Wehrspohn, "Light trapping concepts for photon management in solar cells," *Green* **2**(4), 177–187 (2012).
5. A. S. Dimitrov and K. Nagayama, "Continuous convective assembling of fine particles into two-dimensional arrays on solid surfaces," *Langmuir* **12**, 1303–1311 (1996).
6. A. Mihi, M. Ocana, and H. Miguez, "Oriented colloidal-crystal thin films by spin coating microspheres dispersed in volatile media," *Adv. Mater.* **18**, 2244–2249 (2006).
7. D. Allard, B. Lange, F. Fleischhaker, R. Zentel, and M. Wulf, "Opaline effect pigments by spray induced self-assembly on porous substrates," *Soft Materials* **3**(23), 121–131 (2006).
8. J. Üpping, A. Bielawny, R. B. Wehrspohn, T. Beckers, R. Carius, U. Rau, S. Fahr, C. Rockstuhl, F. Lederer, M. Kroll, T. Pertsch, L. Steidl, and R. Zentel, "Three-dimensional photonic crystal intermediate reflectors for enhanced light trapping in tandem solar cells," *Adv. Mater.* **23**, 3896–3900 (2011).
9. D. J. Norris, E. G. Arlinghaus, L. Meng, R. Heiny, and L. E. Scriven, "Opaline photonic crystals: How does self-assembly work?," *Adv. Mater.* **16**, 1393–1399 (2004).
10. A. Blanco, E. Chomski, S. Grachtak, M. Ibisate, S. John, S. W. Leonard, C. Lopez, F. Meseguer, H. Miguez, J. P. Mondia, G. A. Ozin, O. Toader, and H. M. van Driel, "Large-scale synthesis of a silicon photonic crystal with a complete three-dimensional bandgap near 1.5 micrometers," *Nature* **405**, 437–440 (2000).
11. M. Egen, R. Voss, B. Griesbock, and R. Zentel, "Heterostructures of polymer photonic crystal films," *Chem. Mater.* **15**, 3786–3792 (2003).

12. M. Egen, and R. Zentel, "Surfactant-free emulsion polymerization of various methacrylates: Towards monodisperse colloids for polymer opals," *Macromol. Chem. Phys.* **205**, 1479–1488 (2004).
  13. K. Bittkau, R. Carius, A. Bielawny, and R. B. Wehrspohn, "Influence of defects in opal photonic crystals on the optical transmission imaged by near-field scanning optical microscopy," *J Mater Sci: Mater Electron* **19**, 203–207 (2008)
- 

## 1. Introduction

3D photonic crystals [1,2], such as artificial opals, are a promising material class for the use in advanced light management concepts for solar cells. Their special photonic band structure leads to strong wavelength-dependent and directional reflection and transmission properties which may be exploited in solar cells for innovative angular-selective or energy-selective filters, as well as reflective and diffractive backside structures [3,4]. The optical properties of artificial opals can be designed within a broad range, as opals of many varieties can be easily synthesized experimentally by the self-assembly of monodisperse nanoscaled colloids, without the need for costly instruments [5–7]. The transmission, reflection and photonic dispersion characteristics of the opal are defined by the material and size of the colloids. Inverted opals are of particular interest for the applications mentioned above as they exhibit a complete photonic band-gap. E. g., we recently presented the first successful integration of an inverted opal structure as an intermediate reflective layer in a micromorph tandem solar cells [8]. We could show, that the electrical current of the top cell was significantly enhanced by the 3D photonic crystal structure.

Artificial opals are commonly synthesized from colloidal suspensions. Using conventional methods, either the suspension is drop coated onto the substrate or the substrate is dipcoated into the suspension and subsequently slowly pulled out [9–11]. During the deposition process the substrate is in contact with a reservoir of the colloidal suspension. The crystallization of the opaline film takes place in the meniscus which forms between the liquid phase of the solution and the gas phase of the ambient atmosphere. The combination of the evaporation of the solvent and capillary forces at the substrate surface creates a flow of the suspension which drives the colloids to the crystallization front and advances the crystal growth. However, the disadvantage of the drop and the dip coating fabrication method is their long duration which takes up several hours up to days and the rather small area of the obtained opaline film.

For a successful integration of advanced light management concepts using artificial opals in the photovoltaic industry a low-cost, fast, and large-scale technique to produce extensive opaline films of high quality is needed. The work presented by Zentel *et al.* shows that the fabrication of artificial opals by simply spraying the colloidal suspension onto the substrate is a promising method to comply with these demands [7]. Using a spray coating method enables one to deposit very thin layers of the colloidal suspension onto the substrate. Therefore, the drying process, i. e. the evaporation of the solvent and the concurrent opal crystallization, in principle occurs over the whole area of the substrate simultaneously. This is in contrast to the fabrication methods mentioned above in which the drying process advances along the substrate surface. Thus, the spray coating method offers a huge time saving component compared to the conventional methods. Additionally, this method needs no expensive equipment and obviously can be upscaled easily. However, Zentel *et al.* applied the spray coating process to porous and rather small substrates, such as sheets of paper. Also, they executed the spraying process by manually applying the spraying device, an airbrush, to a sheet of paper. These issues apparently make the application to the solar cell production process impossible in which techniques have to comply with non-porous, smooth as well as textured, and large-area substrates in a controllable and reproducible manner. Here, we report on important upgrades to the approach of Zentel *et al.* and on the successful implementation of an automated process

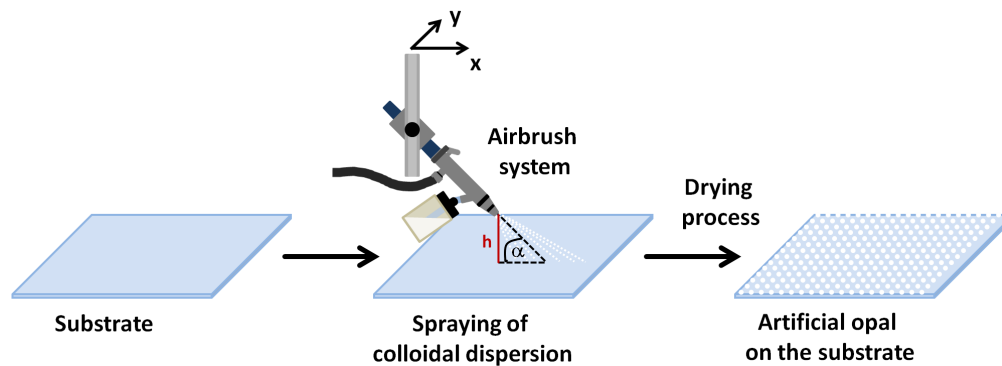


Fig. 1. Schematic illustration of the fabrication process of an artificial opal by spray coating.

for spray-induced self-assembly of extensive artificial opals on non-porous substrates, i. e. glass substrates (size  $15 \times 21 \text{ cm}^2$ ) and aluminium foil. We achieved to reproducibly fabricate opaline films of up to  $10 \times 20 \text{ cm}^2$  prepared on a glass substrate within 1–2 hours. Also, we present a summary on the parameters which influence the resulting opaline films, such as the solid content of the colloidal dispersion, the drying process, the substrate material, and the dispersion agent.

## 2. Materials and methods

The principle of our spray coating process is simple (see Fig. 1). A suspension of highly monodisperse nanoscaled polymethyl methacrylate (PMMA) colloids is sprayed onto the substrate. During the drying sequence the dispersion agent evaporates and the subsequent flow of the agent leads to the crystallization of the opal. As building blocks for the artificial opaline films highly monodisperse PMMA spheres ( $d \approx 240 \text{ nm}$ ) dissolved in deionized water are used. These colloidal dispersions with varying solid content per weight are provided by our project partner Institute of Organic Chemistry at the University of Mainz [12]. The substrates are commercially available glass slides with sizes of up to  $15 \times 21 \text{ cm}^2$  and conventional aluminium foil. As the substrate surface has to be wettable to achieve a uniform distribution of the colloidal dispersion after the spraying process, the substrates need to be pretreated. The glass substrates are treated with a 7M NaOH solution prior to the spraying process, whereas the aluminum foil does not need to be treated as the oxide layer of the untreated foil provides the needed wettability. This effect can be amplified by tempering the aluminum foil at  $300^\circ\text{C}$ , as the thickness of the oxide layer is increased by the tempering.

The experiments were performed using a commercially available airbrush system by Badger to spray the colloidal dispersion onto a substrate. The airbrush device is implemented in a self-constructed apparatus, which mechanically triggers the dispersion flow and the movement of the airbrush in the  $x$ - and  $y$ -direction via a computer software. The distance  $h$  and the angle  $\alpha$  between the substrate and the airbrush can be adjusted (see Fig. 1). We used an angle of  $\alpha = 45^\circ$  and a distance of  $h = 14 \text{ cm}$  for all experiments. The airbrush is moved laterally over the substrate with a velocity of  $9000 \text{ mm/min}$ . The pressure used by the airbrush was set at 1 bar. The drying of the evenly distributed colloidal dispersion on the substrate was performed in an oven under ambient atmosphere.

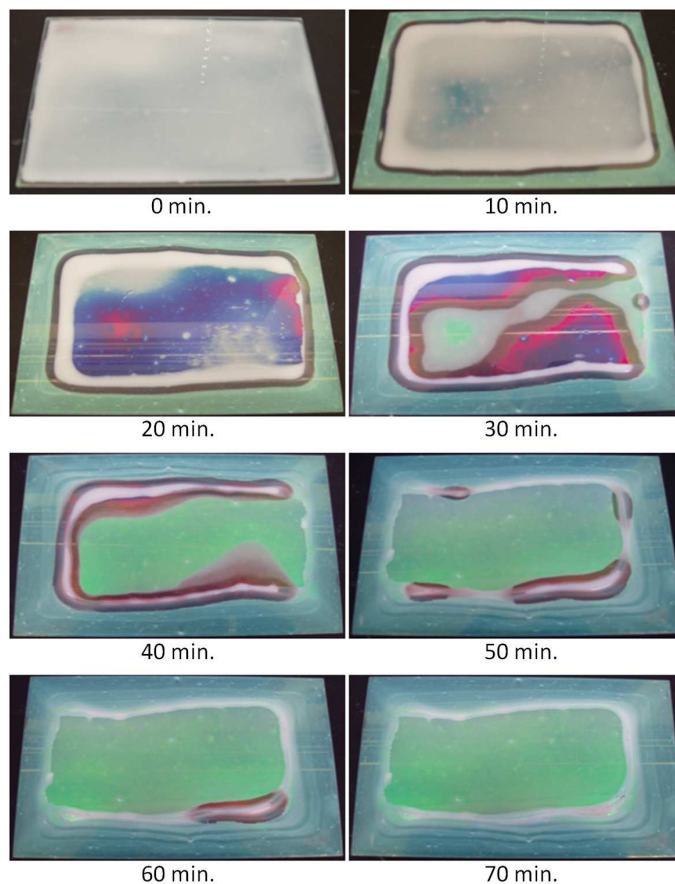


Fig. 2. Course of the drying sequence on a glass substrate. In this example, an approximately  $10 \times 15 \text{ cm}^2$  opal has formed after 70 min. on a  $15 \times 21 \text{ cm}^2$  glass substrate.

### 3. Results and discussion

To achieve artificial opals of high quality via spray coating, process parameters such as the solid content of the colloidal dispersion, the substrate material and the dispersion agent need to be optimized. Most important is the understanding of the drying process, i.e. the evaporation of the solvent and the concurrent opal crystallization, which is strongly affected by the choice of the aforementioned parameters. Therefore, an extensive investigation of the influence of these parameters on the spray coating process was carried out in order to achieve a more precise understanding of the crystallization mechanisms and to gain a better control over the fabrication process of artificial opals on non-porous substrates by spray coating.

#### 3.1. Drying process

The drying process is the most crucial process step during the self-organized crystallization of the artificial opal. The visible course of the drying sequence on a glass substrate is illustrated in Fig. 2. The colloidal dispersion is distributed very evenly on the substrate by the spray deposition (0 min. in Fig. 2). The drying process does not take place simultaneously over the whole substrate as it is the case for porous substrates [7]. The drying rather starts from the

edges of the substrate and then advances to the center (10 min. in Fig. 2). Additionally, there are spots in the central part of the substrate where drying occurs while other parts still seem to be unaffected (20–60 min. in Fig. 2). The evaporation of the dispersion agent and thus the crystallization of the opal takes place at the advancing fronts which form a meniscus between the liquid phase and the ambient air just above the substrate surface. However, the advancing crystallization fronts found here ( $\approx 1$  cm) are laterally much broader than the ones occurring in the conventional fabrication methods ( $\ll 1$  mm), thus leading to quick crystallization durations. After approximately 70 minutes an inner area of approximately  $10 \times 15 \text{ cm}^2$  with high reflectance in the green spectral range and an outer area with low reflectance have formed on the substrate (70 min. in Fig. 2). The optical reflectance of these two distinguishable areas are plotted in Fig. 3 (a) for comparison. The reflectance peaks at around  $\lambda = 535$  nm originate from the photonic stop gap of the artificial opal. While the peak positions are located at the same wavelength, the peak heights differ strongly for the two regions. The reflectance of the inner region achieves a value of  $R \approx 47\%$ , but for the outer region the maximum is at only  $R \approx 18\%$ . SEM cross-sections of these two areas reveal that the PMMA spheres are packed in hexagonal closest packing in the inner area (see Fig. 3 (b)), i. e. an opal has formed, whereas almost no closest packing of the spheres can be detected in the outer area, furthermore the structure here seems to be amorphous (Fig. 3 (c)). Therefore, the synthesized artificial opal is laterally limited to the inner area by the drying process. But in comparison to other fabrication methods on non-porous substrates already an immense upscaling of the opal size was achieved with the automated spray coating presented here.

The drying sequence was examined for different ambient temperatures between  $5^\circ\text{C}$  and  $80^\circ\text{C}$  in an oven, but no influence of the temperature on the resulting opaline films was found. This needs to be investigated further, as it is not understood why the temperature seems not to have an influence on the drying process in these samples.

The contraction of the colloidal dispersion during the drying process additionally leads to the formation of cracks in the artificial opal, which divide the crystal in several microdomains of approximately  $50 \times 50 \mu\text{m}^2$  maximum in size (see Fig. 4). These cracks also occur for other fabrication methods and can not be prevented [13]. However, depending on the proposed design this is not disadvantageous as a certain electrical conductivity of the films often is required when considering possible applications in solar cells. E. g., after inverting opaline films with a suitable filling material the needed conductivity can be provided mainly by these cracks [8].

### 3.2. Solid content of the colloidal dispersion

Colloidal dispersions with concentrations of 19%, 10% and 5% by weight were sprayed onto glass substrates under identical conditions and dried at  $26^\circ\text{C}$  in an oven for 1.5 hours. The resulting opaline films are shown in Fig. 5. The sample which was prepared with the colloidal dispersion of 19% by weight reveals the most even and homogeneous surface with an intense reflectance in the green spectral range (see Fig. 5 (a)). The opaline films prepared with colloidal dispersions of lower concentrations are much more inhomogeneous, i.e. many bright and dark spots are visible within the green reflecting surface. The film which was prepared with the lowest concentration (5%) revealed the lowest quality with the highest number of impurities and crumbs (see Fig. 5 (c)). This sample also has the lowest reflectance and the opaline surface appears stained.

For a quantitative evaluation of the visible appearance reflectance spectra of the opaline films were measured, see Fig. 6 (a). In this graph the reflectance is plotted against the wavelength of light  $\lambda$  for the different concentrations. The spectra were normalized to the reflectance spec-

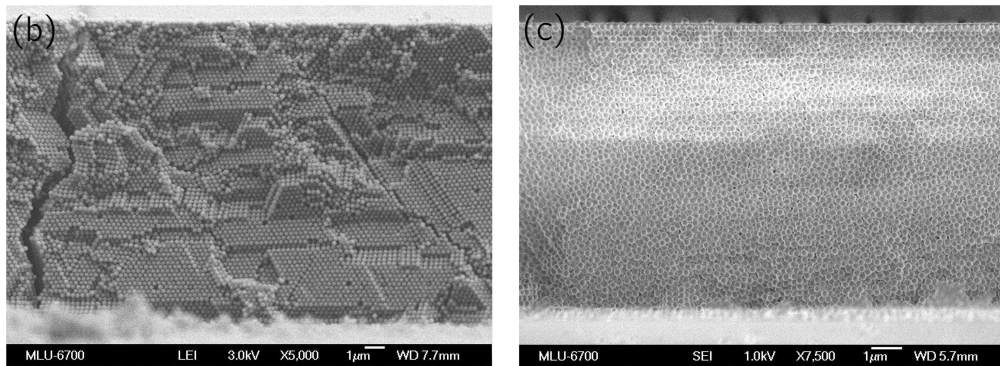
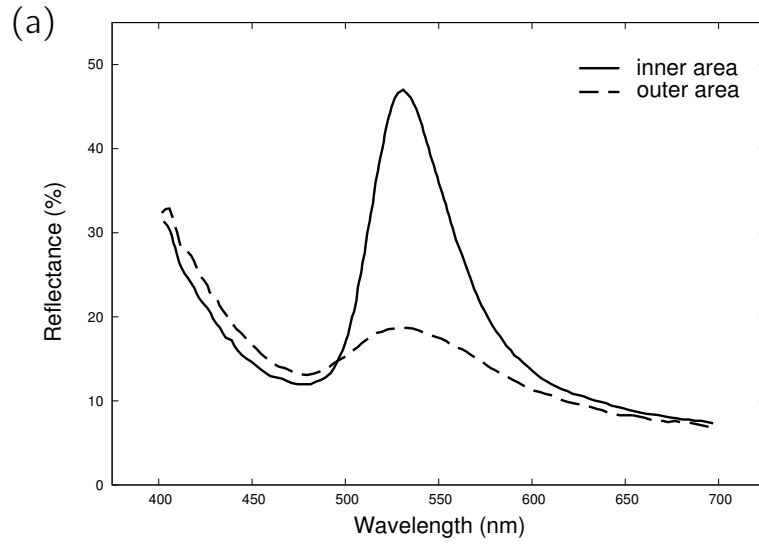


Fig. 3. (a) Reflectance spectra of the spray coating deposited opaline film from the inner (full line) and outer region of the substrate which is presented in Fig. 2. SEM cross-sectional views: Cross-section of the (a) inner region (5000x magnification) and (b) outer region (7500x magnification).

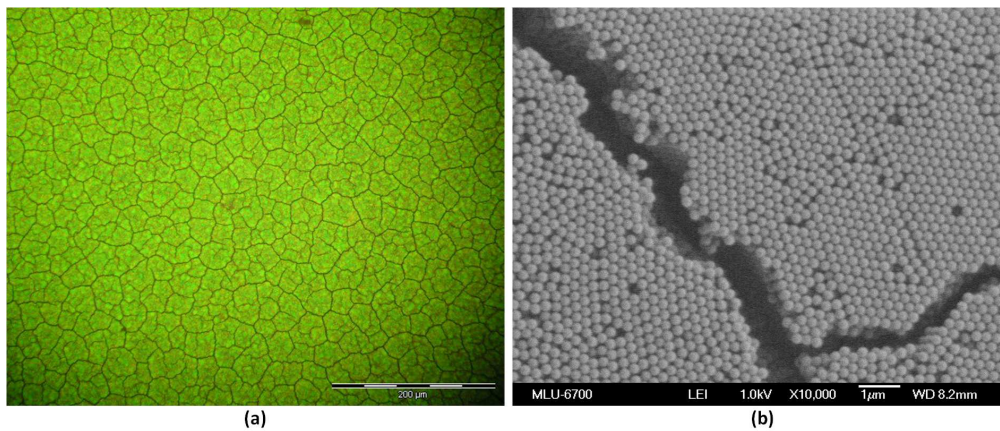


Fig. 4. Cracks in the opaline structure: (a) Optical microscope image in reflection (200x magnification), (b) SEM image (10000x magnification).

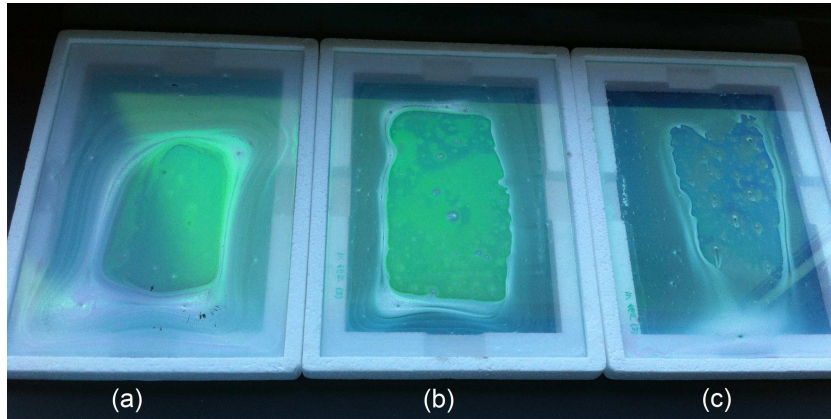


Fig. 5. Samples prepared with different concentrations of the colloidal dispersion: (a) 19%, (b) 10% and (c) 5% by weight.

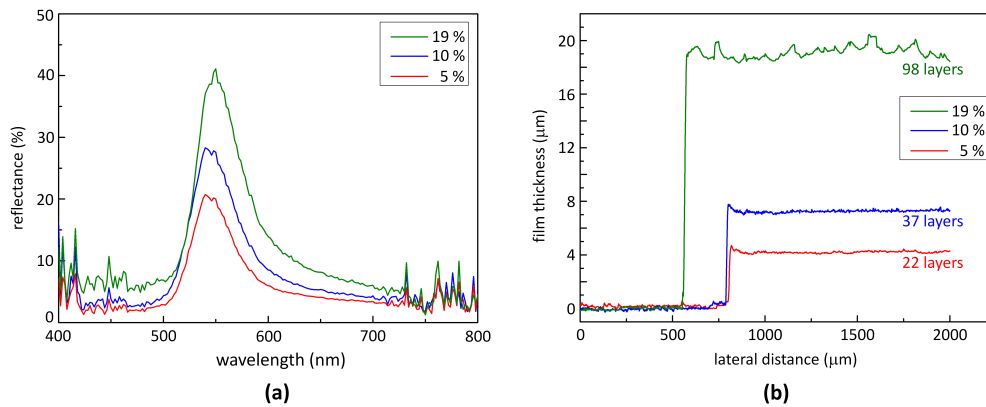


Fig. 6. (a) Reflectance and (b) thickness of the opaline films prepared with colloidal dispersions of varying solid content.

trum of the bare glass substrate. All three samples clearly reveal an increased reflectance in the green spectral range. The spectral position of the peak maximum of the sample which was prepared with the colloidal dispersion of 19% by weight is at a wavelength of  $\lambda = 550\text{nm}$ , whereas the position is slightly shifted to  $\lambda = 548\text{nm}$  for the other samples. The position of the reflectance peaks corresponds to the spectral position of the stop gap of an artificial opal consisting of PMMA spheres with a diameter of 250 nm. We also observe that with an increasing concentration by weight of the colloidal dispersion the maximum peak value of the reflectance rises clearly (see Fig. 6 (a)).

The thickness of the opaline films was determined with the help of a profilometer. A diamond stylus is moved laterally across the sample for a specified distance and a profil of the surface is generated. The opaline film was removed from the substrate at some spots so the edge between opaline film and substrate can be gauged. The film thickness can then be extracted from the diagramm Fig. 6 (b). It was found, that with a higher concentration of the colloidal dispersion, the thickness of the opaline films increases. The opaline film which was prepared with the colloidal dispersion of 19% by weight consists of approximately 98 layers of PMMA colloids on a lateral average. Whereas the opaline film which was prepared with

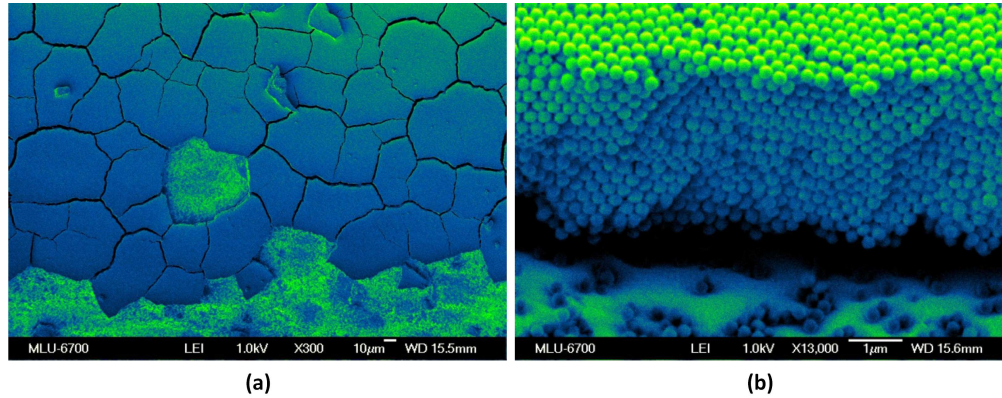


Fig. 7. Artificial opal deposited onto aluminium foil: (a) SEM top view (300x magnification), (b) SEM cross-sectional view (13000x magnification).

the colloidal dispersion of 5% by weight only consists of approximately 22 layers of PMMA colloids. Since the same volume of colloidal dispersion was deposited onto every substrate during the spraying process, the solid content of the colloidal dispersion determines the number of PMMA spheres which arrive on the substrate and compose the crystal. Thus, the thickness of the resulting opaline films is scaled with the content of colloids in the deposited suspension. To fabricate artificial opals of a certain thickness and peak-value of the reflectance the solid content of the colloidal dispersion needs to be adjusted as well as the volume of the deposited colloidal suspensions, e. g. by adjusting the velocity or the pressure of the airbrush.

### 3.3. Substrate material

Also the substrate material has an important influence on the drying mechanisms and thus the resulting opaline films. It has been shown before that for porous substrates, such as sheets of paper, the drying takes place simultaneously over the entire substrate as the dispersion agent is soaked up by the substrate material and the thereby generated liquid flow drives the colloids towards the crystallization front of the opal [7]. However, for non-porous substrates, such as glass substrates, the drying sequence is very different from that of porous substrates. The drying sequence on glass substrates is described in Sec. 3.1. But it remains unclear whether a different non-porous substrate will lead to different results.

Besides on large-area glass substrates we performed first spray coating experiments on conventional commercially available aluminium foil. In contrast to the smooth surface of a glass substrate aluminium foil exhibits a textured surface. The fabrication of 3D photonic crystals on this textured and conducting foil is of potentially high interest for photovoltaic applications. E. g., the aluminium foil may be used as a backside mirror which at the same time acts as an electrical back contact. A photonic crystal structure may add useful light trapping properties to such a backside structure, such as bragg reflection or diffraction.

It was possible to obtain opaline films on aluminium foil substrates, too, which turn out to be very similar to those fabricated on glass substrates. SEM images of the obtained structures are shown in Fig. 7 (a) and (b). Despite the rough texture of the aluminium foil the grown opaline films is crystalline after only a few monolayers and exhibits a smooth top surface. The opaline area is divided into microdomains due to the formation of cracks which is analogue to the case of the deposition onto glass substrates. However, the photonic crystal structures spall very easily from the substrate. On the one hand, this behaviour may

account to a less strong adhesion of the structures to the aluminium foil due to a weaker adhesion strength of the PMMA spheres to the aluminium oxide surface. On the other hand, a possible reason may be that the aluminium foil bends and distorts very easily when handling the samples leading to large mechanical strains inside the opaline structure and subsequent peeling off of the substrate. Because of the high potential of this approach further investigation and optimization of the spray coating deposition process on aluminium foil has to be conducted.

### 3.4. Dispersion agent

In addition, also the dispersion agent has an influence on the drying process. The colloids used in this work are dispersed in deionized water. The high surface tension of this dispersion agent (see Tab. 1) could lead to the observed contraction of the colloidal dispersion during the drying sequence. Therefore, the exchange of the dispersion agent for the PMMA colloids is a good possibility to manipulate the drying process. To fabricate even larger opaline films of similar or better quality, the dispersion agent must have a low surface tension. This property presumably prevents the contraction of the colloidal dispersion during the drying sequence. Also, the vapor pressure of the dispersion agent is an important parameter. If the vapor pressure is too high, i. e. the dispersion agent is very exhalable, the dispersion agent may be in the gaseous phase directly after leaving the airbrush system and before reaching the substrate. Such a property obviously is unfeasible.

Table 1. Surface tension and vapor pressure of several solvents.

	Surface tension at 20° C [mN]	Vapor pressure at 20° C [mbar]
Water	72.75	23
Ethanol	22.55	58
1-Propanol	21.4	20.3
2-Propanol	21.7	42.6
p-Xylene	30	8.89

Ethanol was tested as a dispersion agent because of its low surface tension (see Table 1), but it was found to evaporate too fast. The PMMA spheres do not have enough time to arrange themselves in closest packing. A mixture of ethanol and water leads to the same problems, if the ratio of ethanol is higher than 50%. A higher ratio of water however leads to the known contraction of the colloidal dispersion during the drying sequence. Because of their promising characteristics 1-Propanol and p-Xylene were tested (see Table 1), but were found to corrode the polymethyl methacrylate and thus destroy the spheres. So none of the tested solvents is an applicable dispersion agent. Nevertheless, further experiments showed, that 2-Propanol is a promising candidate, since it does not affect the PMMA spheres, but it needs to be examined further how this solvent effects the drying mechanisms.

### 3.5. Discussion

In comparison to the most common fabrication method for opaline films at present, the dipcoating process, our automated spray coating process presented here offers an immense upscaling of the obtained size of the films (as needed for implementation in solar cells). The size of artificial opals fabricated via dipcoating is technically limited to a few square millimeters, whereas our results suggest that using the automated spray coating, in principle square meter large areas

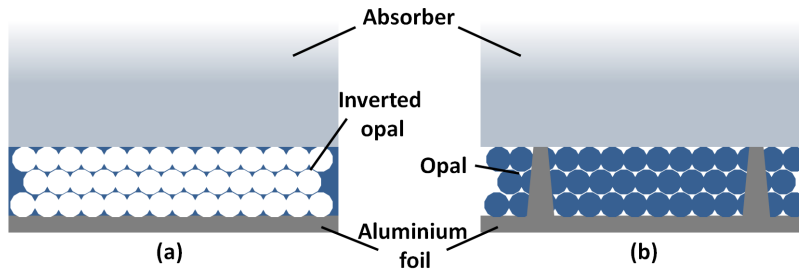


Fig. 8. Possible implementations of a backside foil on solar cells. The backside foil is applied to the backside of the absorber. (a) Photonic crystal structure (here: inverted opal) consists of a electrically conducting material and the foil acts as a large scale backside contact. (b) Photonic crystal structure (here: opal) is isolating, electrical contacts are laser-fired into the absorber material.

of opaline films can be produced. Additionally, artificial opals can be produced much faster via spray coating. The fabrication of an opaline film of  $156 \times 156 \text{ mm}^2$  (size of a conventional solar cell) via dipcoating would require approximately 48 hours (using a pull velocity of 3.25 mm/h). Only 1–2 hours are needed for an opaline film of the same size via spray coating. This is due to the different drying process of the two fabrication methods. In the case of the spray coating the crystallization takes place in multiple, laterally broad fronts ( $\approx 1 \text{ cm}$ ) which start from the edges and advance towards the center of the sample, whereas during the dipcoating the crystallization takes place in just one vertically advancing meniscus ( $\ll 1 \text{ mm}$ ) which leads to much longer fabrication durations.

Imperfections within the crystal structure of the opal possess a crucial impact on the optical quality of the opal as it is apparent from the optical spectra in Fig. 3 (a). Opaline films deposited by our spray coating technique exhibit an area of low quality at the edge region of the substrate which is much larger than that of opals deposited by other methods, e. g. the dip coating technique. However, the extend of this area is not dependent on the absolute size of the substrate except for small substrates with dimensions similar to that of the low quality edge region. Thus, the appearance of low quality areas is not a disadvantage when considering applications involving large-area substrates as it is the case in the photovoltaic industry.

Applying 3D photonic crystals to the backside of a solar cell is a promising light management approach for light path enhancement. Light that is not absorbed during the first round through the solar cell would be either Bragg reflected or diffracted by the photonic crystal structure back into the cell. While the reflection is spectrally broadband, the diffraction is resonant, i. e. spectrally narrow and can be tuned to critical spectral ranges (near the electronic band gap of the absorber material). Therefore, the probability of light absorption and thus the efficiency of the solar cells is increased by such a backside structure [3,4].

Incorporating new concepts, such as light management by opals, directly into existing solar cell production lines involves several drawbacks which the photovoltaic industry commonly is not willing to take. E. g., the preparation of photonic crystals onto a solar cell absorber means an extra process step which is tied to increased production complexity, cost, and time. Also, the probability of defects introduced into the cell is increased because of additional thermal and mechanical exposures.

In the case of a backside structure, we propose that these drawbacks can be avoided by implementing the backside structure as a foil. This backside foil is fabricated in a process which is separate from the solar cell production process. It consists of a flexible substrate and a photonic crystal and is applied to the absorber after its fabrication, e. g. by glue assembly.

The independent fabrication cuts down possible additional damaging impacts on the absorber material. Using aluminium foil as a substrate in combination with our presented spray coating technique for the preparation of opaline films as shown in paragraph 3.3, the proposed backside foil is not limited to a certain type of solar cells. Depending on the desired optical and electrical properties of the backside foil the photonic crystal may be a conventional opal, e. g. as deposited, or an inverted opal, e. g. obtained by atomic layer deposition and subsequent dissolving of the PMMA spheres. Aluminium as a substrate material offers several advantages. It is a low cost metal, it is well-known and already in use in the photovoltaic industry. It acts not only as a substrate for the opaline film but also as a backside mirror for light that was not absorbed in the absorber or bragg reflected or diffracted by the opal structure. Since the proposed backside foil additionally has to act as an electrical backside contact, aluminium as a substrate material is advantageous, too. There are different ways to electrically contact the absorber. If the photonic crystal is made of a transparent electrically conductive material, such as Al:ZnO or ITO, the whole backside foil acts as a large-scale backside contact as sketched in Fig.8 (a). In that case, the formation of cracks in the opaline film as shown in paragraph 3.1 is of great advantage, since they provide a low resistance contact to the absorber. If the opal is electrically isolating, electrical contacts can be achieved by laser-firing the aluminium into the absorber material (see Fig.8 (b)). This strategy enables localized selective electrical contacts if needed and avoids unwanted short-circuits.

#### 4. Conclusion

In conclusion, we presented the fabrication of extensive artificial opals on non-porous smooth and textured substrates, such as glass substrates and aluminium foil, by a low-cost, automated spray coating process. In addition to an immense time saving, a large upscaling of the opal size was achieved in comparison to other fabrication methods on non-porous substrates. We obtained opaline films of up to approximately  $10 \times 15 \text{ cm}^2$  within fabrication durations of approximately 70 min. The size limiting process is the drying sequence, which leads to the formation of an opal in the inner region of the substrate and a not closest packed formation of the spheres at the outer regions of the substrate. The investigated parameters solid content of the sprayed colloidal dispersion, substrate material, and dispersion agent have been shown to play an important role in the spray coating process influencing properties of the opaline films such as thickness, lateral size, optical properties, and overall quality. Using optimized values of these parameters will enable one to even increase the achieved lateral dimensions of the opal and precisely control its properties. For the incorporation of advanced light management concepts with 3D photonic crystals into innovative solar cell devices we propose the use of a backside foil which is applied to the absorber. This foil is made of an aluminium foil substrate and an opaline film deposited with the spray coating method. The backside foil is fabricated in a separate process step, thus making this concept feasible for the photovoltaic industry.

#### Acknowledgments

This work has been carried out by the Infravolt-Consortium. Financial support by the German Federal Ministry of Education and Research (BMBF) within the projects Infravolt and Struktur-solar is gratefully acknowledged (as well as the German Science foundation within the project PAK 88 Nanosun). We like to thank our partners from the Research consortium for stimulating discussions in particular the Institute of Organic Chemistry at the Johannes Gutenberg-University Mainz.

We thank Sabrina Lehmann and Julia-Maria Osinga for their experimental assistance and Claudia Stehr and Susanne Wille for their excellent technical support.